

Identification of pre-breakdown mechanism of silicon solar cells at low reverse voltages

Dominik Lausch,^{1,a)} Kai Petter,² Ronny Bakowskie,² Christian Czekalla,³ Jörg Lenzner,³ Holger von Wenckstern,³ and Marius Grundmann³

¹Mikrostrukturdiagnostik und Analytik, Fraunhofer-Center für Silizium-Photovoltaik (CSP), Walter-Hülse-Str. 1, D-06120 Halle (Saale), Germany

²R&D Silicon, Q-Cells SE, OT Thalheim, Sonnenallee 17-21, D-06766 Bitterfeld-Wolfen, Germany

³Fakultät für Physik und Geowissenschaften, Institut für Experimentelle Physik II, Universität Leipzig, Linnéstr. 5, D-04103 Leipzig, Germany

(Received 15 June 2010; accepted 27 July 2010; published online 20 August 2010)

The local breakdown of commercial silicon solar cells occurring at reverse voltages of only 3–4 V has been investigated by means of current-voltage measurements, dark lock-in thermography, and reverse-biased electroluminescence (ReBEL) with a spatial resolution on the micrometer-scale. It is shown that the origin of the local breakdown (so-called type I) can be traced back to a contamination of the wafer surface with Al particles prior to the phosphorous diffusion step. A model is presented explaining that the spectral maximum of ReBEL is within the visible range. © 2010 American Institute of Physics. [doi:10.1063/1.3480415]

Solar cells in modules are reverse biased when they are shaded.¹ This can lead to diode breakdown, eventually destroying the module by thermal degradation. Hence, electrical breakdown of multicrystalline (mc) silicon solar cells is a relevant technological problem; it limits the number of cells within a string of a module. The ideal planar n^+p junction with a net doping concentration of about $p \approx 10^{16} \text{ cm}^{-3}$ exhibits a breakdown voltage U_r beyond 60 V.² However, in real mc-Si solar cells the breakdown occurs often below 13 V. To avoid this early breakdown it is of particular importance to understand its reasons and mechanisms, especially with regard to the development of the utilization of silicon with lower quality. It is known that such low breakdown voltages are due to local prebreakdown which can be classified into three types according to the I–U characteristic.^{3–5} Highest prebreakdown voltages ($U_r > 14 \text{ V}$) are attributed to field enhancement at etch pits in regions of nonrecombination active bulk defects by Bauer *et al.*³ and are labeled type III. Type II prebreakdown ($10 \text{ V} < U_r < 13 \text{ V}$) is attributed to regions with high density of recombination active bulk defects in the underlying silicon wafer.⁴ Both, type II and type III prebreakdown sites emit light under reverse bias and the position of these sites corresponds to that of bulk defects as recently demonstrated by reverse-biased electroluminescence with spatial resolution on the micrometer-scale (μ -ReBEL).⁶ Despite the progress in characterization and understanding of prebreakdown sites of type II and type III, the origin of prebreakdown of type I, showing much lower breakdown voltages of 5 V and below, remained puzzling.

In this work, we report on visible electroluminescence (EL) at specific and localized sites exhibiting prebreakdown voltages of about 3 V corresponding to prebreakdown of type I. Similar EL was already reported for many silicon-based systems by several authors.^{7–9} For instance Li *et al.*¹⁰ observed light emission from thin Si-rich SiO_x film onto n^+ -type and p -type Si substrates. They propose light emission due to radiative recombination of electron–hole pairs via

defect levels located in the SiO_x layer. Here we unambiguously demonstrate that the type I prebreakdown sites are due to aluminum stains forming a local metal-insulator-semiconductor (MIS) diode.

The samples analyzed are mc-Si solar cells fabricated with a commercial process based on B-doped ($p \approx 10^{16} \text{ cm}^{-3}$) $156 \times 156 \text{ mm}^2$ mc-Si wafers. The wafers were texturized with KOH (alkaline texture) revealing the (111) facets; crystal defects are not delineated. After the anisotropic etching the n -type emitter is realized on the front side of the wafer by phosphorus diffusion. Subsequently a silicon nitride film is deposited serving as an antireflection coating. Finally, front (silver paste) and back (aluminum paste) contacts are printed onto the wafers. Subsequently, the contacts are fired for 10 min into the wafer at a temperature of about 850 °C.

Spatially resolved and spectrally integrated EL intensity images of these solar cells were acquired with a Si charge-coupled device (CCD) camera. For investigations on the micrometer scale a Si CCD camera was mounted onto a Carl Zeiss microscope. The EL spectra were recorded with a microphotoluminescence setup.¹¹ The setup allows spatially and spectrally resolved EL measurements. The spatial resolution is about 1 μm . We used a FEI Nova NanoLab 200 to prepare cross-sections with the focused Ga ion beam; for energy dispersive x-ray (EDX) spectroscopy we used the high-resolution field emission secondary electron microscope. The acceleration voltage for the EDX measurement was 15 keV.

Spectrally integrated EL images of reverse-biased solar cells (ReBEL) clearly reveal the positions of prebreakdown sites. For reverse voltages of about $U_r = 13 \text{ V}$ local breakdown occurs at numerous sites which can be correlated with prebreakdown at bulk defects.⁶ For a reverse bias of $U_r = 4 \text{ V}$ ($I = 37 \text{ mA}$) light emission is not detectable for type II and type III prebreakdown sites. However, there are a few sites emitting light in the visible part of the electromagnetic spectrum. The emitted light is visible to the naked eye. These spots are also detectable by dark lock-in thermography mea-

^{a)}Electronic mail: dominik.lausch@esp.fraunhofer.de.

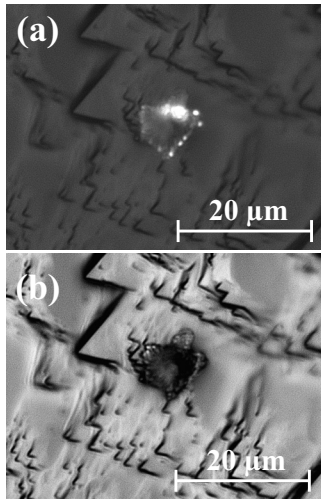


FIG. 1. (a) μ -ReBEL images of light emitting spots recorded for a reverse bias of $U_r=3$ V. The reflected-light microscopy images (b) proof here that the position of light emission (a) corresponds to that of a stain.

measurements using $U_r=4$ V (not shown here). Such defects were denoted as type I by various authors.³⁻⁵ The I-U characteristic of the solar cell investigated in this study does not reveal strong ohmic shunts and no global prebreakdown behavior at $U_r=4$ V. Notably the influence of type I prebreakdown sites on the global I-U characteristic is very small. The physical origin of this type of prebreakdown was so far unclear.

We investigated various type I sites in higher magnification using μ -ReBEL. Figure 1(a) shows such a typical site. By comparing the μ -ReBEL image with the surface morphology depicted in the photomicrograph in Fig. 1(b) it is obvious that the position of light emission corresponds to the position of a stain. For the recording of Fig. 1(a) we used a reverse bias of only 3 V in order to precisely locate the position of light emission. The light escapes preferentially at the borders of the stain [cf. Fig. 1(a)]. It is, however, not clear if light is generated beneath the stain and subsequently absorbed. However, we suggest that the mechanism responsible for the luminescence occurs particularly at the borders of the structure.

In order to determine the spectral distribution of the luminescence arising from the stain spectrally resolved EL measurements were performed at different reverse voltages for the stain shown in Fig. 1. For each voltage applied ($3\text{ V} < U_r < 10\text{ V}$) the spectral distribution was similar. The spectrum recorded for $U_r=6$ V is shown exemplarily in Fig. 2. The spectrum exhibits a broad band ranging from 400 nm beyond 800 nm having its maximum at about 715 nm. The maximum of the luminescence intensity arising from the stains is maximal in the visible range, hence the luminescence is visible to the naked eye. This is in contrast to luminescence for type II and III sites which exhibit a spectral maximum in the near-infrared. A linearly increasing intensity of the measured spectrum with increasing reverse voltages was observed for the whole band. No spectral shift is noticeable. To clarify the origin and the prebreakdown mechanism of type I prebreakdown sites chemical analysis was performed in plane-view and cross-section.

Figure 3 shows a secondary electron microscopy (SEM) image of the stain of Fig. 1. EDX mapping was performed in

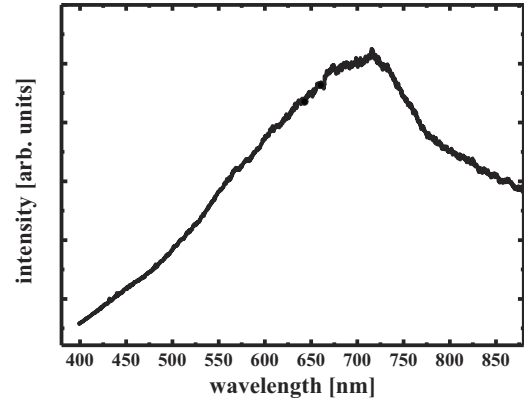


FIG. 2. Spectrally and spatially resolved EL measurement of a stain (type I). The spectrum exhibits a broad band ranging from 400 nm beyond 800 nm having its maximum at about 715 nm.

plane-view (Fig. 3) and cross section (Fig. 4). Aluminum and oxygen are located only at the position of the stain. Notably the borders where the light is emitted from are covered by silicon nitride clearly visible in Fig. 3 depicting the intensity of the characteristic nitrogen core level energy. Figure 4 shows an EDX mapping of the cross-section of the same stain investigated in Fig. 1 and Fig. 3. Also here the nitrogen signal corresponding to the silicon nitride layer is visible. Please note that the aluminum and oxygen signal is located clearly beneath the silicon nitride visible by comparing the nitrogen and oxygen maps.

We conclude that the stain is due to aluminum oxide on top of the p-n diode. It must have been on the device before the deposition of the silicon nitride antireflection layer and before contacting. This provides strong evidence that the aluminum oxide is also penetrating the phosphorus-doped emitter of the solar cell. The oxidation and diffusion are caused by high temperature processes (see Fig. 5). If processed with the same production line, such kind of breakdown is also observed for monocrystalline silicon solar cells (not shown here). Typically, breakdown of monocrystalline silicon solar cells at voltages about $U_r=4$ V can often attributed to type I prebreakdown. Thus we conclude that type-I prebreakdown sites are due to contamination of the wafer with aluminum particles before and during processing, respectively.

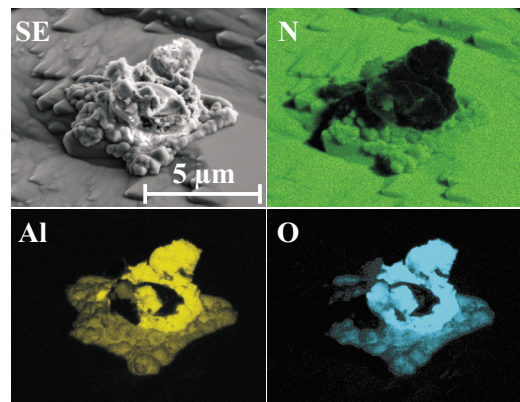


FIG. 3. (Color online) EDX mapping and SE image of the stain of Fig. 1. The aluminum and the oxygen are clearly located at the position of the stain. Notably the borders where the light is emitted from are covered by silicon nitride.

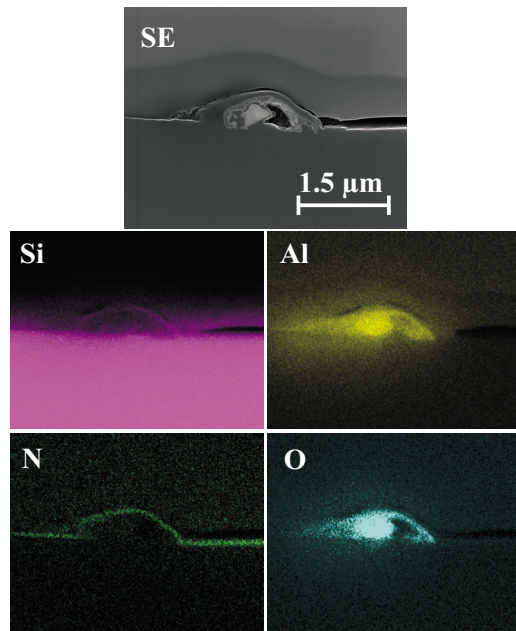


FIG. 4. (Color online) EDX mapping and SE image of the stain of Fig. 1. The aluminum and the oxygen are clearly located at the position of the stain. Notably the borders where the light is emitted from are covered by silicon nitride.

Light emission from silicon is very inefficient due to the fact that silicon has an indirect band structure. Furthermore, light emission due to radiative band–band recombination would not occur in the visible range. Despite of this, several authors have reported efficient light emission from Si structures at energies above its fundamental band gap.^{7–9} In the case of porous silicon and some nanosilicon structures, it is widely accepted that visible light emission is attributed to band–band recombination of electron–hole pairs in nanometer-sized silicon particles. Quantum confinement effect causes the shift in the EL maximum toward higher energies.¹²

The EL spectrum of Fig. 2 is similar to spectra recorded for metal/SiO_x/Si heterostructures.¹⁰ There, light emission is

due to radiative recombination of electron–hole pairs via defect levels located in the SiO_x layer. The spectrum is in principal the same for metal/SiO_x/p-Si and metal/SiO_x/n⁺-Si junction, however, the mechanism of hole injection is different. As result light emission is observed for both cases only, if positive voltage is applied to the Si (forward-biased solar cell for the case of p-Si emitter and reverse-biased solar cell for the case of n-Si emitter). For our samples light emission at Al stains occurs under reverse bias (the positive voltage is applied to the n⁺-Si) and suggests that it originates at a metal/SiO_x/n⁺-Si junction. We suggest that the aluminum stain is on the surface of the p-Si wafer already before the solar cell process. There it will likely form a good Ohmic contact to the p-Si base (cf. Fig. 5), hence the p-Si base and the Al stain have the same electrical potential. During realization of the emitter a thin SiO_x-layer is formed between emitter and the aluminum stain, schematically visualized by the blue line in Fig. 5(b). Therefore, the MIS-diode consists of the Al stain acting as the metal, SiO_x as insulator and the n-Si emitter being the semiconductor. The proposed model explaining the emission of visible light in the vicinity of an Al stain might also be true for light emission observed close to Al particles using the same polarity but voltages of $U_r = 10$ V.¹³

The proposed model explains the following: (i) light emission is observed for reverse bias only, (ii) light emission originates in the vicinity of the oxidized Al stain, (iii) the spectral distribution of the emitted light, and (iv) prebreakdowns of type I are not “strong” Ohmic shunts.

In summary, prebreakdown sites of type I emitting visible light can clearly be attributed to aluminum stains. We have confirmed this for randomly chosen seven stains in total from mc-Si wafers all showing the behavior as reported in this letter. These stains adhere on the wafer before the deposition of the silicon nitride antireflection layer and before contacting. The emitted light is a result of radiative recombination of electron–hole pairs via defect levels located in the thin SiO_x layer between the n⁺-emitter and the aluminum stain.

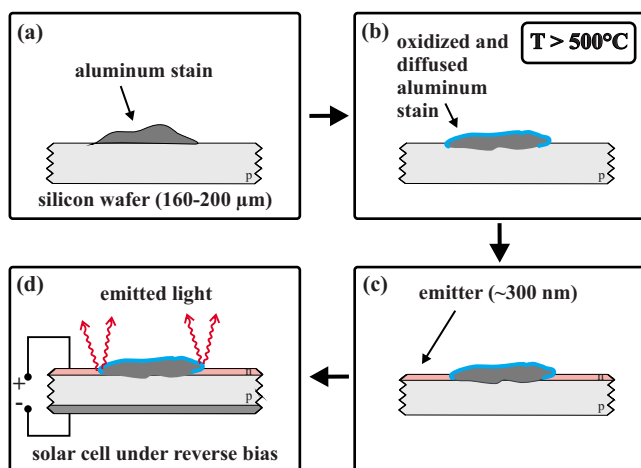


FIG. 5. (Color online) Scheme of the formation of the MIS diode between an aluminum stain, a thin SiO_x-layer and the n⁺-emitter of the solar cell. (a) The p-type wafer with aluminum stain, (b) oxidized aluminum stain, (c) wafer with emitter, and (d) finished solar cell. The light emitted from the borders of the structure is indicated by the red serpentine lines.

¹A. Woyte, J. Nijs, and R. Belmans, *Sol. Energy* **74**, 217 (2003).

²S. M. Sze and G. Gibbons, *Appl. Phys. Lett.* **8**, 111 (1966).

³J. Bauer, J.-M. Wagner, A. Lotnyk, H. Blumtritt, B. Lim, J. Schmidt, and O. Breitenstein, *Phys. Status Solidi (RRL)* **3**, 40 (2009).

⁴W. Kwapil, M. Kasemann, P. Gundel, M. C. Schubert, W. Warta, P. Bronsveld, and G. Coletti, *J. Appl. Phys.* **106**, 063530 (2009).

⁵K. Bothe, D. Hinken, K. Ramspeck, S. Herlufsen, J. Schmidt, R. Brendel, J. Bauer, J.-M. Wagner, N. Zakharov, and O. Breitenstein, *J. Appl. Phys.* **106**, 104510 (2009).

⁶D. Lausch, K. Petter, H. von Wenckstern, and M. Grundmann, *Phys. Status Solidi (RRL)* **3**, 70 (2009).

⁷S. Lazarouk, V. Bondarenko, S. La Monica, G. Maiello, G. Masini, P. Pershukovich, and A. Ferrari, *Thin Solid Films* **276**, 296 (1996).

⁸G. F. Bai, Y. Q. Wang, Z. C. Ma, W. H. Zong, and G. G. Qin, *J. Phys.: Condens. Matter* **10**, L717 (1998).

⁹X. M. Wu, Y. M. Dong, L. J. Zhuge, C. N. Ye, N. Y. Tang, Z. Y. Ning, W. G. Yao, and Y. H. Yu, *Appl. Phys. Lett.* **78**, 4121 (2001).

¹⁰A. P. Li, G. F. Bai, K. M. Chen, Z. C. Ma, W. H. Zong, Y. X. Zhang, and G. G. Qin, *Thin Solid Films* **325**, 137 (1998).

¹¹C. Czekała, J. Lenzner, A. Rahm, T. Nobis, and M. Grundmann, *Superlattices Microstruct.* **41**, 347 (2007).

¹²J. Yuan and D. Haneman, *J. Appl. Phys.* **86**, 2358 (1999).

¹³O. Breitenstein, J. P. Rakotoniaina, M. H. Al Rifai, and M. Werner, *Prog. Photovoltaics* **12**, 529 (2004).